

Techno-economic assessment of coal- or biomass-fired oxy-combustion power plants with supercritical carbon dioxide cycle

Xiaoyu Wei, Vasilije Manovic, Dawid P. Hanak*

*Energy and Power, School of Water, Energy and Environment,
Cranfield University,
Bedford, Bedfordshire, MK43 0AL, UK*

*Corresponding author: *Dawid P. Hanak, d.p.hanak@cranfield.ac.uk*

Abstract

Oxy-fuel combustion is regarded as a feasible technology that can contribute towards decarbonisation of the power industry. Although it has been shown that oxy-fuel combustion results in lower carbon dioxide emissions at a lower cost of carbon dioxide captured compared to the mature amine scrubbing process, its implementation still results in high economic penalties. This study proposes to replace the conventional steam cycle in the state-of-the-art oxy-combustion coal-fired power plants with the supercritical carbon dioxide cycle to reduce both economic and efficiency penalties. In addition, in order to further reduce carbon dioxide emissions, biomass is considered as a replacement fuel for coal in the oxy-fuel combustion power plant and the proposed process becomes a type of bio-energy with carbon capture and storage. The process models were developed in Aspen Plus™ to assess techno-economic feasibility of the considered processes. The results showed that on replacement of the conventional steam cycle with the supercritical carbon dioxide cycle, the efficiency penalties were reduced by up to 2% points and the levelised cost of electricity was reduced up to 4.6% (4.1 €/MWh). Moreover, when biomass was used as a fuel, the net efficiency penalties increased by 0.5% points and the levelised cost of electricity increased by 24.4 €/MWh. Although techno-economic performance in this case was less favourable under no carbon tax conditions, using biomass resulted in significant negative carbon dioxide emissions (-3.70 megatonnes of carbon dioxide per annum). Such negative emissions can offset carbon dioxide emissions from other sources that are relatively difficult to decarbonise. If the carbon tax is above 24 € per tonne of carbon dioxide, bio-energy with carbon capture and storage became more economically feasible than fossil fuel with carbon capture and storage.

Key Words: oxy-fuel combustion, supercritical carbon dioxide Brayton cycle, bio-energy and carbon capture and storage, process modelling, techno-economic assessment, feasibility assessment

NOMENCLATURE

AC	Cost of CO ₂ avoided	€/tCO ₂
A_{HE}	Heat exchange surface area	m ²
BEC	Bare erected cost	M€
C_C	BEC of the supercritical CO ₂ compressor	M€
C_{CT}	BEC of the cooling tower	M€
C_{CW}	BEC of cooling water system	M€
C_{cycle,CO_2}	BEC of the sCO ₂ power cycle	M€
C_E	BEC of the sCO ₂ expander	M€
C_{EG}	BEC of the electric generator	M€
C_{HE}	BEC of the heat exchanger	M€
CF	Capacity factor	%
$e_{CO_2,capture}$	Specific CO ₂ emission of the power plant with CCS	gCO ₂ /kW _{el} h
$e_{CO_2,ref}$	Specific CO ₂ emission of the power plant without CCS	gCO ₂ /kW _{el} h
e_{CO_2}	Specific CO ₂ emission	gCO ₂ /kW _{el} h
HHV	Higher heating value	MJ/kg
$i_{p\&c}$	Piping and integration cost indicator	%
$LCOE$	Levelised cost of electricity	€/MW _{el} h
$LCOE_{capture}$	Levelised cost of electricity with CCS	€/MW _{el} h
$LCOE_{ref}$	Levelised cost of electricity without CCS	€/MW _{el} h
$\dot{m}_{CO_2,Com/Exp}$	Equivalent mass flow rate of CO ₂ at the inlet to the compressor/expander	kg/s
$\dot{m}_{AE,Com/Exp}$	Equivalent mass flow rate of air at the inlet to the compressor/expander	kg/s
\dot{m}_{CO_2}	CO ₂ emission rate	g/a
\dot{m}_{fuel}	Mass flow rate of the fuel	kg/s
$p_{AE,out}$	Equivalent air outlet pressure	bar
p_{HE}	Highest pressure of the heat exchanger	bar
p_{in}	Expander/compressor inlet pressure	bar
P_{ASU}	ASU power consumption	MW _{el}
P_{CPU}	CPU power consumption	MW _{el}
P_{FAN1}	Flue gas circulation fan power consumption	MW _{el}
P_{FAN2}	Main fan power consumption	MW _{el}
P_G	Gross power output	MW _{el}
$\sum P_{AUX}$	Total power consumption of the auxiliary equipment	MW _{el}
\dot{Q}_{CW}	Heat duty of the cooling water system	MW _{el}
SFC	Specific fuel cost	€/MW _{el} h
T_{in}	Expander inlet temperature	°C
TCR	Total capital requirement	M€
VOM	Variable operating and maintenance cost	M€
\dot{W}_{net}	Net power output	kW _{el}
$\eta_{i,Com}$	Compressor isentropic efficiency	%
$\eta_{i,Exp}$	Expander isentropic efficiency	%
η_{net}	Net efficiency	%
$\rho_{in,Air}$	Air density at the inlet of compressor/expander	kg/m ³
ρ_{in,CO_2}	CO ₂ density at the inlet of compressor/expander	kg/m ³
ρ_{out,CO_2}	CO ₂ density at the outlet of compressor/expander	kg/m ³

$\rho_{out,Air}$

Air density at the outlet of compressor/expander

kg/m³

ABBREVIATIONS

ASU	Air separation unit
ANL	Argonne National Lab
BECCS	Bio-energy with carbon capture and storage
BFPP	Biomass-fired power plant
CCS	Carbon capture and storage
CFPP	Coal-fired power plant
COP	Compressor outlet pressure
CPU	Compression and purification unit
DECC	Department for Energy and Climate Change
EOR	Enhanced oil recovery
ETS	Emission Trading Scheme
GCRA	Gas-Cooled Reactor Associates
HVAC	Heating, ventilation and air conditioning
IBDP	Illinois Basin Decatur Project
ICLAS	Integrated chemical looping air separation unit
IEA	International Energy Agency
IFRF	International Flame Research Foundation
IL-ICCS	Illinois Industrial CCS
IPCC	Intragovernmental Panel on Climate Change
NETL	National Energy Technology Laboratory
ORNL	Oak Ridge National Laboratory
Oxy-CLAS	Oxy-fuel combustion with chemical looping air separation
SC	Steam cycle
sCO ₂	Supercritical carbon dioxide
TEA	Techno-economic analysis
TIT	Turbine inlet temperature
UNFCCC	United Nations Framework Convention on Climate Change
WP	Wood pellet

1 Introduction

The International Energy Agency (IEA) has recently reported that anthropogenic greenhouse gas emissions have resulted in a global mean temperature increase of about 1°C above pre-industrial levels, of which more than 0.3°C was caused by carbon dioxide (CO₂) emissions from coal combustion [1]. At the current rate of anthropogenic greenhouse gas emissions, the global mean temperature increase will reach 1.5°C by around 2040 [2]. This is mostly because global energy-related CO₂ emissions rose by 1.7% to an all-time high of 33.1 GtCO₂, driven by rising energy demand associated with growth in the global economy by 3.7% in 2018 [1]. Regardless of such an increase in CO₂ emissions, the global coal demand increased for the second year in a row. However, the role of coal in the global energy portfolio continued to decline. This is evident from the annual growth rate of 0.7% in 2018 that was significantly lower than that of 4.5% between 2000 and 2010. While coal's share in primary energy demand and power generation continues to decline slowly, it remains the largest source of electricity and the second-largest source of primary energy [1]. Therefore, development of advanced low-carbon coal-fired power plants is essential to meet the emission reduction targets.

Carbon capture and storage (CCS) is considered a key technology to reduce emissions from energy and carbon-intensive industries, as it is expected to reduce industrial CO₂ emissions by 50% by 2050 [3]. Importantly, it has been shown that if CCS is not considered in the decarbonisation scenario, the cost of achieving the CO₂ emission reduction targets could rise up to 140% [4]. Oxy-fuel combustion, as one of the main CCS technologies, is a process in which fuel is burnt in an oxygen-rich environment rather than in air. To control the flame temperature in the combustor, high-purity (95%_{vol}) oxygen (O₂), which is produced in an air separation unit (ASU) and contains the balance of nitrogen (N₂) and argon (Ar), is diluted with a part of the recycled flue gas. With combustion under this O₂-rich and N₂-lean atmosphere, the main components of the flue gas are CO₂ and water vapour (H₂O). As a result, a concentrated CO₂ stream is produced after water vapour condensation, and subsequent conditioning in a compression and purification unit (CPU) for permanent storage (CCS) or utilisation (CCU).

In the early 1980s, the combustion of fuels in a mixture of high-purity O₂ and recirculated flue gas was proposed to obtain a high-purity CO₂ stream for enhanced oil recovery (EOR) [5] and to reduce the CO₂ emissions from fossil fuel power generation [6]. In the following decades, small-scale experimental studies were conducted by the Argonne National Lab (ANL) [7], the International Flame Research Foundation (IFRF) [8], the IHI Corporation [9], and CANMET [10]. Furthermore, supporting fundamental studies have been performed to compare oxy-fuel combustion with air combustion with respect to the characteristics of fuel [11], boiler performance [12] and flue gas composition [13]. Since 2000, global research activities have increased the number of demonstration phase projects. However, due to the technical barriers, associated mainly with the high energy-intensity of the ASU, commercial operation of oxy-fuel combustion technology has been delayed [14]. Since 2010, several major pilot plants and pre-commercial demonstration projects have been operated worldwide to prove the technical feasibility of oxy-fuel combustion technology. All pilot and demonstration projects in operation are less than 100 MW_{th} in capacity. Most projects focus only on research into the CO₂ capture process, such as those in Germany (30 MW_{th} [15]), the USA (15 MW_{th} [16] and 30 MW_{th} [17]), the United Kingdom (40 MW_{th} [18]), France (30 MW_{th}), and Australia (30 MW_{th} [19]). The Callide Oxyfuel project demonstrated that CCS technology can be applied to coal-fired power plants, generating electricity with virtually no emissions, and became the world's first retrofitted industrial-scale demonstration of oxy-fuel combustion, which was available to be applied to commercial-scale

capture-ready power plants and could be scaled to above 350 MW_{el} [20]. CanmetENERGY (formerly CANMET) is currently working on hydroxy-fuel combustion (the 3rd generation oxy-fuel system) in which fuel is burnt in a high-purity O₂ environment without flue gas recirculation, using water or steam as a temperature moderator [14]. The advantage of this configuration is that it reduces capital cost by reducing the mass flow of gas in the system. Yet, novel turbomachinery needs to be developed and driven by steam/gas mixtures as a working medium.

Cormos [21] evaluated the performance of oxy-fuel combustion power plants fired with coal, lignite and sawdust. Their study showed that the considered process would result in efficiency penalties of 9-12% points, compared to the reference coal-fired power plant without CCS. The major challenge of oxy-fuel combustion is a high efficiency penalty resulting from the high-purity O₂ production in the ASU (50-60%) and CO₂ compression in the CPU (30-40%), which together account for approximately 90% of the energy penalty [21,22]. This has resulted in 50–95% increase in the LCOE. Singh et al. [23] compared the techno-economic performance of amine scrubbing and oxy-fuel combustion retrofitted to an existing coal-fired power plant. Both processes were shown to increase electricity prices by up to 20–30% compared with the reference coal-fired power plant without CCS. However, oxy-fuel combustion was shown to be more attractive due to its lower CO₂ emissions and lower cost of CO₂ capture. Overall, it is reported in the literature that the levelised cost of electricity (LCOE) of oxy-coal combustion using coal is between 70 €/MW_{el}h [21] and 106.3 €/MW_{el}h [24], and using sawdust is 78.87 €/MW_{el}h [21]. Therefore, development of options to reduce the energy requirement of oxy-fuel combustion and improve its economic performance is essential for this technology to become feasible and deployed at scale. Zhou et al. [25] considered an integrated chemical looping air separation unit (ICLAS) to address the challenge of the high power requirement of the cryogenic-based ASU. Their study proved ICLAS using steam and recycled flue gas significantly enhanced the techno-economic performance of the oxy-fuel combustion power plant and showed that application of ICLAS can reduce the efficiency penalty of oxy-fuel combustion from 9.5% to 5% and can reduce the LCOE by up to 20%.

In addition to CCS, bio-energy with CCS (BECCS) is one of the CO₂ removal technologies that has been considered as crucial to achieving the emission reduction targets set by the Intragovernmental Panel on Climate Change (IPCC) [2]. This is because negative-emission technologies, such as BECCS, are expected to contribute towards stabilising global-mean temperature increase at a low level in the future. The concept of BECCS is based on the fact that biomass absorbs CO₂ from the atmosphere as it grows. If CO₂ is then captured and stored after the combustion of biomass, CO₂ is permanently removed from the atmosphere and BECCS is characterised with negative CO₂ emissions. Therefore, BECCS feasibility would benefit from the emission trading scheme (ETS). As of 2019, six projects were in operation capturing CO₂ from ethanol bio-refinery plants and municipal solid waste recycling centres, and five BECCS projects have been cancelled due to the difficulty of obtaining planning permission and their unfavourable economic feasibility. The predecessor of the Illinois Industrial CCS (IL-ICCS) project, the Illinois Basin Decatur Project (IBDP), successfully captured and stored 1 MtCO₂ over a 3+ year timeframe [26]. However, other planned and existing BECCS projects are significantly smaller. In February 2019, the Drax Power Station started operation of their innovative BECCS plant with the first CO₂ being captured using C-Capture technology with capture capacity 1 tCO₂/day [27]. While the number of existing and planned projects is promising, if BECCS is to make a significant contribution to meeting CO₂ reduction targets, hundreds of such projects are needed worldwide.

The major challenges of BECCS are the low efficiency and high LCOE resulting from the lower energy density and higher biomass price compared to that of coal, which hinder deployment of BECCS. Moreover, the deployment of BECCS is limited by the availability of sustainable biomass, CO₂ storage capacity and energy intensity of CCS [28]. Al-Qayim et al. [29] have confirmed that application of oxy-fuel combustion to BECCS is more economically feasible than application of post-combustion CO₂ capture. Their study showed that the efficiency of the oxy-fuel combustion power plant fired with wood pellets was 3.8% points higher than that for the same power plant with post-combustion CO₂ capture (26.4%). Moreover, the LCOE was 6% lower in the oxy-fuel combustion case (~160 €/MW_{el,h}). Yet, this figure was nearly double that for oxy-fuel combustion using coal (~86 €/MW_{el,h}).

It is important to emphasise that the studies on oxy-fuel combustion in the CCS and BECCS applications relied on a conventional steam cycle for power generation. However, the recent trend in power generation, especially for solar and nuclear power plants, suggests that application of a closed-loop Brayton cycle using supercritical carbon dioxide (sCO₂) as the working medium is one of the most promising energy conversion technologies. This is because it can achieve >5% higher cycle efficiencies than the conventional steam cycle [30]. It also offers a more compact structure, a lower construction cost and a smaller footprint [31]. In 1968, Angelino [32] and Feher [30] first demonstrated that the closed Brayton cycle with sCO₂ as the working medium and using a small amount of compression work at the optimal circulating temperature could result in a higher conversion efficiency. In addition, the research of Gokhstein et al. [33] was crucial in the early development of the sCO₂ cycle as they demonstrated its potential feasibility in nuclear power plants. It needs to be stressed that assessment of the economic feasibility of the sCO₂ cycle is challenging, as the cost estimation and economic model are based only on empirical formulas and reference models. Dostal [34] performed an economic assessment of the sCO₂ cycle [35] and compared its economic performance with that of the steam cycle and helium cycle using the relevant data of the Gas-Cooled Reactor Associates (GCRA) [36]. Their study showed that the capital cost of the sCO₂ cycle can be up to 24% lower than the conventional steam cycle and 7% less expensive than the helium Brayton cycle.

This study aimed to demonstrate that replacement of the conventional steam cycle in state-of-the-art oxy-fuel combustion power plants with the sCO₂ cycle can reduce economic and efficiency penalties associated with oxy-fuel combustion. It also aimed to assess the techno-economic feasibility of such oxy-fuel combustion power plants when biomass is used as a fuel, alleviating the challenges of BECCS. To evaluate the thermodynamic performance of the proposed oxy-fuel combustion power plants, the process models of the considered cases were developed in Aspen Plus™. Furthermore, the economic feasibility of replacing the conventional steam cycle with the sCO₂ cycle for efficient conversion of energy from oxy-fuel combustion was evaluated considering coal and biomass as fuel. Following an initial techno-economic assessment, a sensitivity analysis was performed to understand the effect of the key design assumptions on the feasibility of the considered cases. The economic performance was characterised in terms of LCOE and cost of CO₂ avoided. The feasibility of the final cases was then benchmarked against the reference oxy-fuel combustion power plant with the conventional steam cycle.

2 Process description

In this work, a 660 MW_{el, gross} oxy-fuel coal-fired power plant (CFPP) developed by Hanak et al. [22] was considered as the reference case. Based on the reference case, technical retrofits and improvements

were considered to explore opportunities for reduction in efficiency and economic penalties. The detailed descriptions for the reference and retrofitted cases are described in Section 2.1 and Section 2.2, respectively.

2.1 Reference oxy-fuel combustion coal-fired power plant with a supercritical steam cycle

The reference oxy-fuel combustion CFPP consists of a once-through boiler, a supercritical steam cycle with a single reheat and a flue gas treatment system. Under base-load operation, superheated steam of 537°C and 235 bar is raised in the oxy-fuel combustion boiler, which drives a high-pressure steam turbine with an outlet pressure of 45.2 bar. Steam is then reheated to 554°C in the boiler and subsequently drives the intermediate- and low-pressure steam turbines. The feedwater heating train comprises five low-pressure feedwater heaters and three high-pressure feedwater heaters to maximise steam cycle efficiency. The last low-pressure feedwater heater, called the deaerator, is a mixed feedwater heater.

It is assumed that O_2 is supplied at 95%_{vol} purity from a cryogenic ASU with a specific power requirement of 200 kW_{el}/tO₂. Moreover, two-thirds of the flue gas from the oxy-combustion of coal is recycled to maintain combustion conditions in the chamber similar to that of the reference air-combustion case. After mixing with O_2 from the ASU, the concentration of O_2 in the mixed gas for coal combustion is fixed at 27%_{vol}. The excess air and air leakage into the boiler are 20%_{vol} and 2%_{vol}, respectively. This results in CO₂ concentration of more than 60%_{vol} in the flue gas, with the balance being H₂O and trace amounts of O_2 , N₂, and Ar. The flue gas is then purified in the CPU which comprises a double-flash separation unit with internal cooling, to remove H₂O and the non-condensable species, thereby satisfying conditions for CO₂ transport and storage, 110 bar and over 90%_{vol} CO₂ purity [22]. To ensure a fair comparison between the cases analysed in this study, the work recovery system proposed by Hanak et al. [22] is not considered.

Table 1: Summary of the key process assumptions

Parameter		Value
Oxy-combustion coal-fired power plant		
Boiler	Design excess air ratio (% _{vol, dry}) [22]	20.0
	Design air leakage (% _{vol, wet}) [22]	2.0
	Discharge pressure of the induced draft fan (bar) [22]	1.05
	Discharge pressure of the forced draft fan (bar) [22]	1.11
	Isentropic efficiency of fans (%) [22]	75.0
	Mechanical efficiency of fans (%) [22]	100.0
	Recycled flue gas ratio (%) [22]	64.8
sCO ₂ cycle system	Design O ₂ content in oxidising medium (% _{vol, wet}) [22]	30.0
	Initial turbine inlet temperature (°C) [37]	650
	Initial turbine outlet pressure (bar) [37]	250
	Isentropic efficiency of the sCO ₂ turbine (%) [37]	0.93
	Isentropic efficiency of the compressor (%) [37]	0.85
	Mechanical efficiency of the sCO ₂ turbine and the compressor (%) [37]	0.99
	Design discharge temperature of the cooler (°C) [37]	31.25
Auxiliary equipment	Design discharge pressure of the cooler (bar) [37]	7.4
	Generator	Electrical efficiency (%) [37]
	CO ₂ purification	
	compression unit	
		Polytropic efficiency of CO ₂ compressors (%) [22]
		Mechanical efficiency of CO ₂ compressors (%) [22]
		Isentropic efficiency of CO ₂ pump (%) [22]
Air separation unit		Intercooling temperature (°C) [22]
		CO ₂ initial compression pressure (bar) [22]
		CO ₂ final pressure (bar) [22]
		CO ₂ temperature at inlet pump (°C) [22]
		ASU specific power (kW _{el} /tO ₂) [38]
		O ₂ purity (% _{vol}) [22]
		Polytropic efficiency of air compressors (%) [22]
		Intercooling temperature (°C) [22]
		Final air pressure (bar) [22]

2.2 Technical retrofit and performance improvement

The retrofitted oxy-fuel combustion power plants (Figure 1) were modelled in Aspen Plus™ based on the oxy-fuel combustion boiler from the reference oxy-fuel CFPP. The thermodynamic properties were estimated using the Peng Robinson cubic equation of state with the Boston-Mathias alpha function (PR-BM) for the oxy-fuel combustion, ASU and CPU. The PR-BM was selected as it is recommended for hydrocarbon applications. Moreover, the Lee-Kesler-Plöcker equation of state (LK-PLOCK) was used to accurately represent the CO₂ properties under supercritical conditions in the sCO₂ power cycle. The main assumptions for the cases considered in this work are presented in Table 1.

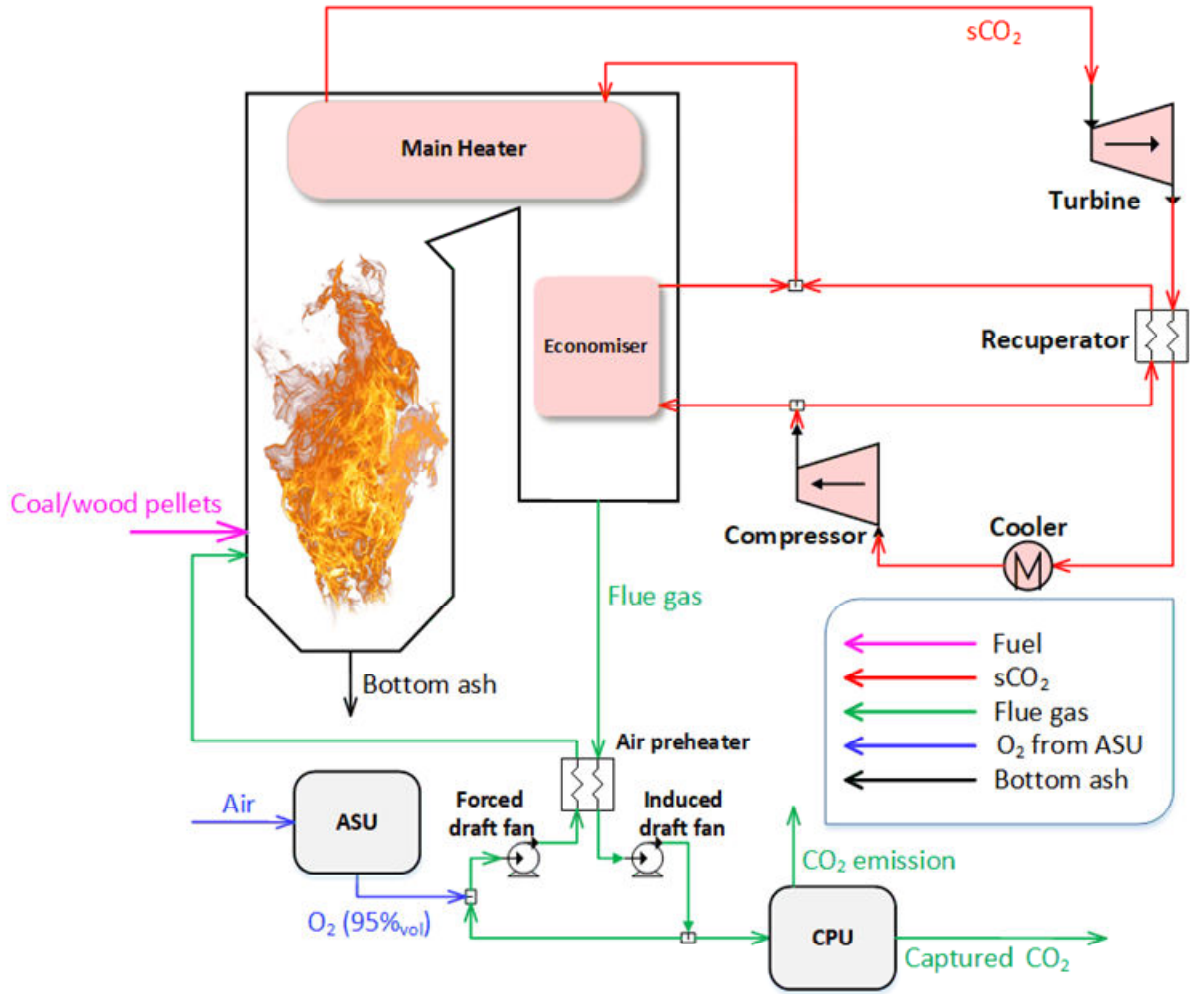


Figure 1: Retrofitted oxy-fuel power plant flow diagram

The $s\text{CO}_2$ cycle is a closed recuperated $s\text{CO}_2$ Brayton cycle with one $s\text{CO}_2$ turbine, one compressor and one recuperator. In the integrated system, the low-temperature, low-pressure CO_2 is compressed to 250 bar in the compressor. It is then divided into two streams that are preheated by two different heat sources. The first stream is preheated by the flue gas stream at the exit of the boiler. The second stream is preheated by the CO_2 stream discharged from the $s\text{CO}_2$ turbine. Both streams are then mixed and further heated in the oxy-fuel combustion boiler to 650°C [37], as assumed in Table 1. The high-pressure, high-temperature $s\text{CO}_2$ stream is then expanded in the turbine, which subsequently drives the generator to produce power. As a result, the temperature and pressure of the $s\text{CO}_2$ stream leaving the turbine are about 519°C and 77 bar, respectively. These are further reduced to 31°C and 74 bar, above the critical point for CO_2 , in the recuperator and the cooler. The solid fuels considered in this work are coal (South African bituminous coal) [39] and biomass (wood pellet, WP) [40] with the compositions presented in Table 2. Based on the above considerations, the following cases are further investigated:

- SC-coal case – Oxy-fuel combustion CFPP with supercritical steam cycle.
- $s\text{CO}_2$ -coal case – Oxy-fuel combustion CFPP with $s\text{CO}_2$ cycle.
- $s\text{CO}_2$ -WP case – Oxy-fuel combustion biomass-fired power plant (BFPP) with $s\text{CO}_2$ cycle.

Table 2: Fuel composition

Parameter	Coal [39]	Wood pellets [40]
Ultimate analysis		
Carbon (%wt, dry basis)	69.80	46.96
Hydrogen (%wt, dry basis)	3.58	6.86
Nitrogen (%wt, dry basis)	1.73	0.26
Oxygen (%wt, dry basis)	7.66	44.43
Sulphur (%wt, dry basis)	0.55	0.21
Ash (%wt, dry basis)	16.68	1.28
Proximate analysis		
Ash (%wt, dry basis)	16.68	1.28
Volatiles (%wt, dry basis)	22.85	85.00
Fixed carbon (%wt, dry basis)	60.47	13.72
Moisture (%wt)	2.44	5.34
Higher heating value (MJ/kg)	26.74	17.02

3 Techno-economic assessment methods

The oxy-fuel combustion cases considered in this work have been characterised considering their thermodynamic and economic performance. The methodology employed for the techno-economic assessment, developed based on the work by Hanak et al. [22], was further refined in this work considering the work of Ciferno et al. [41] and Michalski et al. [42], as presented in detail in Section 3.1 and Section 3.2.

3.1 Thermodynamic assessment

To evaluate the thermodynamic performance, the process models for the considered oxy-fuel combustion power plant cases have been built in Aspen Plus™. One of the important indicators is the net efficiency of the entire power plant (η_{net}), which is the ratio of the net output power of the entire power plant and heat input from fuel combustion, as shown in Eq. (1). The net power output of the power plant is the difference between the gross power output (P_G) generated by the generator driven by a turbine, and the total power consumption of the auxiliary equipment ($\sum P_{AUX}$) in the power plant. The heat input from fuel combustion was obtained by the product of mass flow rate of the fuel (\dot{m}_{fuel}) and higher heating values (HHV) of the fuel that was estimated by the Dulong formula [43].

$$\eta_{net} = \frac{P_G - \sum P_{AUX}}{\dot{m}_{fuel} \cdot HHV} \quad (1)$$

In this study, $\sum P_{AUX}$ in Eq. (2) comprises the induced draft fan (P_{FAN1}), forced fan (P_{FAN2}), ASU power consumption (P_{ASU}) and CPU power consumption (P_{CPU}).

$$\sum P_{AUX} = P_{FAN1} + P_{FAN2} + P_{ASU} + P_{CPU} \quad (2)$$

In the context of global efforts to reduce emissions, specific CO₂ emission (e_{CO_2}) is used as the environmental performance indicator. The specific CO₂ emission (e_{CO_2}) is estimated using Eq. (3) and is defined as the ratio of CO₂ emission rate (\dot{m}_{CO_2}) and the net output power of the power plant (\dot{W}_{net}).

$$e_{CO_2} = \frac{\dot{m}_{CO_2}}{\dot{W}_{net}} \quad (3)$$

3.2 Economic assessment

The economic performance of the proposed cases is compared with the reference oxy-fuel CFPP [22]. The LCOE is commonly employed to estimate the cost of electricity shown as Eq. (4) [22]. It is a function of total capital investment, fuel cost, operating and maintenance costs and discount rate. The LCOE is defined as the ratio of the total cost and the total power output of the power plant during its lifetime, including total capital requirement (TCR), fixed charge factor (FCF), fixed operating and maintenance cost (FOM), capacity factor (CF), variable operating and maintenance cost (VOM) and specific fuel cost (SFC), which considers the lifetime of the power plant and project interest rate. The FCF is calculated as a function of discount rate (r) and the project lifetime (t) in Eq. (5). It is worth noting that the cost associated with CO₂ emission is accounted for in the VOM as the product of carbon tax and annual CO₂ emission rate.

$$LCOE = \frac{TCR \times FCF + FOM}{\dot{W}_{net} \times CF \times 8760} + VOM + \frac{SFC}{\eta_{net}} \quad (4)$$

$$FCF = \frac{r(1+r)^t}{(1+r)^t - 1} \quad (5)$$

Another economic performance indicator, the cost of CO₂ avoided (AC, Eq. (6)), is also considered [22]. It compares a plant with CCS to a reference plant without CCS [41] and quantifies the average cost of avoiding a unit of atmospheric CO₂ emissions while providing a unit of electricity [44].

$$AC = \frac{LCOE_{capture} - LCOE_{ref}}{e_{CO_2,ref} - e_{CO_2,capture}} \quad (6)$$

The capital cost of the power plant is calculated using the economic data from the reference power plant (Table 3) through the exponential method function [45]. The main difference between the considered cases is the type of power cycle. Therefore, the total capital cost of the power cycle and the cooling water system need to be recalculated in the cases that consider sCO₂ cycle. This is achieved using Eq. (7) that consider the bare erected costs (BEC, M€), engineering, construction management, home office and fees (Eng'g CM H.O. & Fee, M€), process contingency (Process Cont., M€) and project contingency (Project Cont., M€) [41].

$$TCR = BEC + Eng'g \text{ CM H.O. \& Fee} + Process \text{ Cont.} + Project \text{ Cont.} \quad (7)$$

As there is no reliable data source for the sCO₂ cycle, Eq. (8) is used to estimate the BEC. This depends on the BECs of the supercritical CO₂ compressor (C_C), CO₂ expander (C_E), four heat exchangers (ΣC_{HE}), electric generator (C_{EG}) and cooling tower (C_{CT}), and the piping and integration cost indicator ($i_{P\&C}$).

$$C_{cycle,CO_2} = (1 + i_{P\&C}) \cdot (C_C + C_E + \Sigma C_{HE} + C_{EG} + C_{CT}) \quad (8)$$

The supercritical CO₂ compressor and the expander are two main unit operations of such cycle. Their BECs are estimated using the methodology developed by Benjelloun et al. [46] shown in Eq. (9). The BEC of the supercritical CO₂ compressor is determined by the equivalent air mass flow rate ($\dot{m}_{AE,Com}$),

compressor isentropic efficiency ($\eta_{i,Com}$), compressor inlet pressure (p_{in}) and equivalent air outlet pressure ($p_{AE,out}$).

$$C_C = \dot{m}_{AE,Com} \cdot \frac{47.1}{1 - \eta_{i,Com}} \cdot \frac{p_{AE,out}}{p_{in}} \cdot \ln\left(\frac{p_{AE,out}}{p_{in}}\right) \quad (9)$$

In terms of the BEC of the CO₂ turbine, it depends on the equivalent air mass flow rate ($\dot{m}_{AE,Exp}$), expander isentropic efficiency ($\eta_{i,Exp}$), expander inlet pressure (p_{in}) and equivalent air outlet pressure ($p_{AE,out}$) (Eq. (10)). The constant 392.2 was derived based on the results from Criado, Arias and Abanades [47], and Gabbrielli and Singh [48].

$$C_E = \dot{m}_{AE,Exp} \cdot \frac{392.2}{1 - \eta_{i,Exp}} \cdot \frac{p_{in}}{p_{AE,out}} \cdot \ln\left(\frac{p_{in}}{p_{AE,out}}\right) \cdot [1 + \exp(0.036 \cdot T_{in} - 65.66)] \quad (10)$$

To calculate $\dot{m}_{AE,Com/Exp}$, the volume flow rate of air and CO₂ at the inlet of the compressor and the expander were assumed to be equal, and the mass flow rate is proportional to the density, as shown in Eq. (11). Assuming that the outlet volumetric flow rate of CO₂ and air are also the same, the outlet air density ($\rho_{out,Air}$), in the case of equivalent outlet air pressure of the compressor and the expander, are derived (Eq. (12)).

$$\dot{m}_{AE,Com/Exp} = \dot{m}_{CO_2,Com/Exp} \cdot \frac{\rho_{in,Air}}{\rho_{in,CO_2}} \quad (11)$$

$$\rho_{out,Air} = \frac{\dot{m}_{AE,Com/Exp}}{\dot{m}_{CO_2,Com/Exp}} \cdot \rho_{out,CO_2} \quad (12)$$

To obtain the air density, the corresponding equivalent outlet pressure was determined using an iterative process. It needs to be highlighted that all calculations performed in this work with Eq. (11) and (12) used the real gas database (CoolProp) [49].

The BECs of heat exchangers (C_{HE}) including a superheater, recuperator, economiser, and cooler were estimated using Eq. (13) which depends on the heat exchange surface (A_{HE}) and highest pressure of the heat exchanger (p_{HE}). The BEC of the electric generator (C_{EG}) used the gross power output of the generator (P_G) as the scaling factor in Eq. (14) [50].

$$C_{HE} = 2546.9 \cdot A_{HE}^{0.67} \cdot p_{HE}^{0.28} [\text{€}] \quad (13)$$

$$C_{EG} = 84.5 \cdot P_G^{0.95} [\text{€}] \quad (14)$$

The BEC of the cooling water system (C_{CW}) was determined considering its unit cost and heat duty (\dot{Q}_{CW}) as presented in Eq. (15). The unit cost of the cooling water system was set to 32.3 €/kW [41].

$$C_{CW} = 32.3 \dot{Q}_{CW} [\text{€}] \quad (15)$$

Furthermore, it is assumed that the process contingency is zero. Estimations of Eng'g CM H.O. & Fee and Project Contingency (M€) for the considered cases were determined using proportions based on their respective BECs shown in Table 3. Also, since feedwater and miscellaneous balance of plant systems are not applicable in the proposed cases, these are not accounted for in the TCR. It is assumed that the variable operations and maintenance (O&M) yearly cost rate is 2.0% of TCR and fixed O&M yearly cost rate is 1.0% of TCR. The fixed charge factor, which is defined as a ratio used to calculate

the present value of an annuity, is around 10% without considering salvage value, tax and depreciation [51]. The base year for economic calculation was 2018. It is also assumed that the variable costs are constant over time in real terms.

Table 3: Economic model assumptions

Parameter	Value
Reference oxy-fuel combustion power plant	
Reference total plant cost (M€) [52]	1302.2
Reference gross power output (MW) [52]	785.9
Reference total steam cycle cost (M€) [52]	120.3
Bare erected cost (M€) [52]	98.6
Engineering, Construction Management, Home Office & Fees [52]	9.1 (9.23% of BEC)
Project contingency (M€) [52]	12.5 (12.70% of BEC)
Reference total feedwater & misc. BOP systems cost (M€) [52]	78.1
Bare erected cost (M€) [52]	61.6
Engineering, Construction Management, Home Office & Fees (M€) [52]	5.6 (9.33% of BEC)
Project contingency (M€) [52]	10.9 (14.84% of BEC)
Reference cooling water system cost (M€) [52]	35.9
Scaling factor [52]	0.67
Other economic parameters	
Variable O&M yearly cost rate (%) [53,54]	2.0
Fixed O&M yearly cost rate (%) [53,54]	1.0
Carbon tax (€/t) [53,54]	0.0
Specific CO ₂ transport and storage cost (M€/a) [22]	7.0
Fuel price (€/GJ)	Bituminous (South Africa) [39] 2.8
	Wood Pellets [40] 4.5
Lifetime (years) [53,54]	25
Real discount rate (%) [53,54]	8.78
Annuity factor (%) [53,54]	10.0
Year time (hours) [53,54]	8760
Capacity factor (%) [53,54]	80

4 Results and discussion

In the techno-economic assessment, the net efficiency of the power plant, the specific CO₂ emissions, LCOE and AC were considered as the key performance indicators. Furthermore, identification of the optimum parameters of the working medium, such as raising the turbine inlet temperature (TIT) and the compressor outlet pressure (COP), is one way to improve the net efficiency and reduce the costs associated with CCS. Moreover, the economic performance depends upon the assumptions made in the analysis. It is pertinent to assess the effect of the carbon tax, fuel price, and discount rate on LCOE and AC. Therefore, this work analysed the effect of these parameters on the techno-economic performance of the cases identified above. The initial working medium parameters in the sCO₂ cycle cases are 650°C and 250 bar [37], and the remaining assumptions are shown in Table 2 and Table 3. The sensitivity analysis was performed to evaluate the effect of TIT, COP, carbon tax, fuel price, and discount rate on the techno-economic performance of the considered cases by varying:

- TIT between 500–900°C [55];

- COP between 100–300 bar;
- Carbon tax between 0–140 €/t;
- Fuel price by $\pm 25\%$; and
- Discount rate between 1.0–15.0%.

4.1 Thermodynamic assessment

The analysis of the thermodynamic performance (Table 4) revealed that the net efficiency of the SC-coal case decreased by 10.25%_{HHV} points, with respect to the conventional CFPP with a net efficiency of 38.80%_{HHV}, validated by Hanak et al. [22]. The net efficiency in the sCO₂-coal and the sCO₂-WP cases decreased by 10.70%_{HHV} points and 13.02%_{HHV} points, respectively. In these cases, the net power output decreased by 7.33 MW_{el} and 45.22 MW_{el}, respectively, with respect to the SC-coal case. This corresponds to energy penalties of 1.57%_{HHV} and 9.70%_{HHV}. It needs to be highlighted that the considered structure of the sCO₂ cycle is significantly less complex than that of the conventional steam cycle in the reference case. Its operating conditions need to be further optimised to improve the net efficiency of the sCO₂-coal case. However, a higher net efficiency penalty in the sCO₂-WP case is primarily due to the fuel characteristics of biomass. As a result, optimisation of the sCO₂ cycle conditions may not result in a significant reduction of the net efficiency penalty in the sCO₂-WP case.

Table 4: Summary of the thermodynamic performance

Parameter	Unit	SC-coal case	sCO ₂ -coal case	sCO ₂ -WP case
Chemical energy consumption	MW _{th}	1632.97	1632.97	1632.97
Boiler heat-exchange efficiency	% _{HHV}	89.56	92.45	79.99
Auxiliary electricity requirements				
Condensate pump	MW _{el}	0.63	0.00	0.00
O ₂ -rich stream compressor (the forced draft fan)	MW _{el}	1.49	3.73	4.05
Flue gas booster (the induced draft fan)	MW _{el}	5.27	7.11	6.69
Coal/Wood Pellets handling and pre-treatment, flue gas treatment trains	MW _{el}	11.25	11.39	18.13
Cooling water pump	MW _{el}	2.21	2.29	2.18
Plant auxiliary equipment electricity consumption	MW _{el}	20.85	24.52	31.05
Plant control systems, lighting, HVAC*, steam turbine auxiliaries, transformer losses	MW _{el}	5.00	4.95	4.71
ASU power consumption	MW _{el}	94.06	89.38	89.38
CPU power consumption	MW _{el}	73.37	74.62	75.67
System performance indicators				
Gross power output	MW _{el}	659.45	652.26	621.77
Total auxiliary electricity consumption	MW _{el}	193.28	193.46	200.81
Net power output	MW _{el}	466.17	458.79	420.96
Gross electric efficiency	% _{HHV}	40.38	39.94	38.08
Net electric efficiency	% _{HHV}	28.55	28.10	25.78
Specific fuel consumption	g/kW _{el} h	465.75	479.14	830.99
CO ₂ emission rate	kg/s	11.73	11.40	-146.78
Annual CO ₂ emission rate	MtCO ₂ /a**	0.30	0.29	-3.70
Specific CO ₂ emission	gCO ₂ /kW _{el} h	90.61	89.49	-1255.21
Net efficiency penalty	% _{HHV}	10.25	10.70	13.02

*HVAC: Heating, Ventilation and Air Conditioning

** Refers to CO₂ emission rate per annum

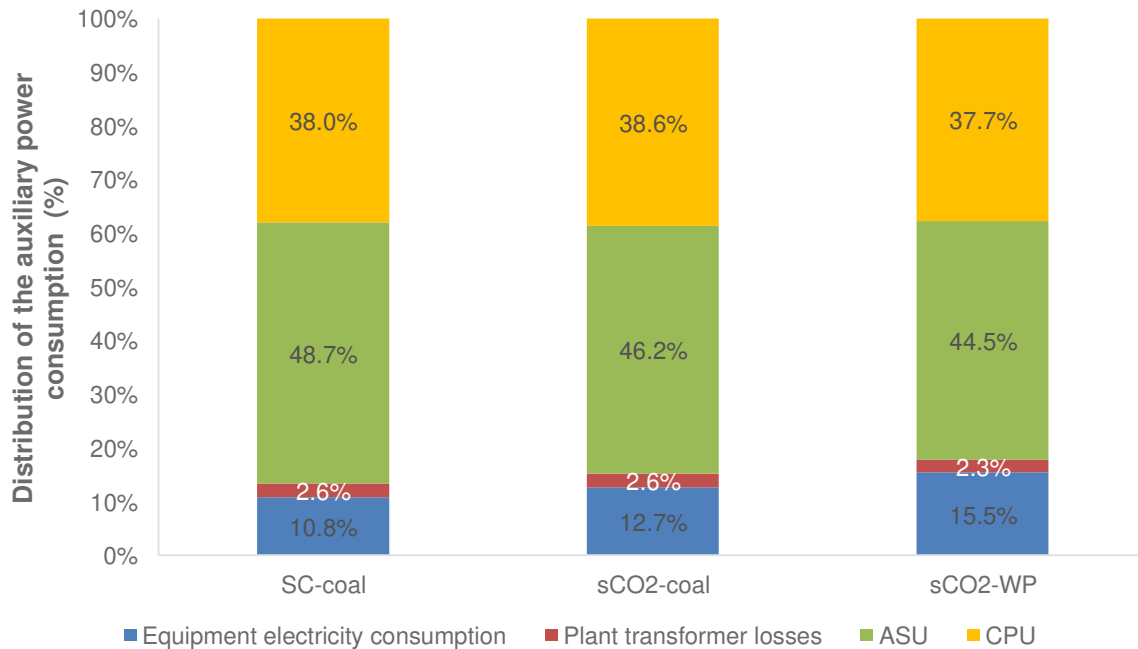
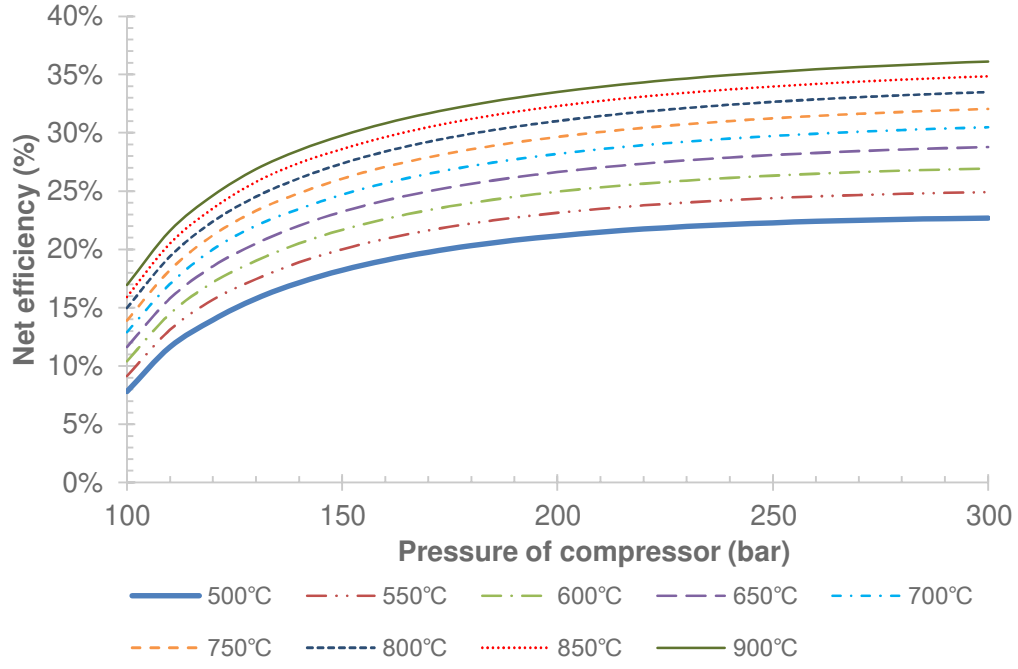


Figure 2: Distribution of the auxiliary power consumption

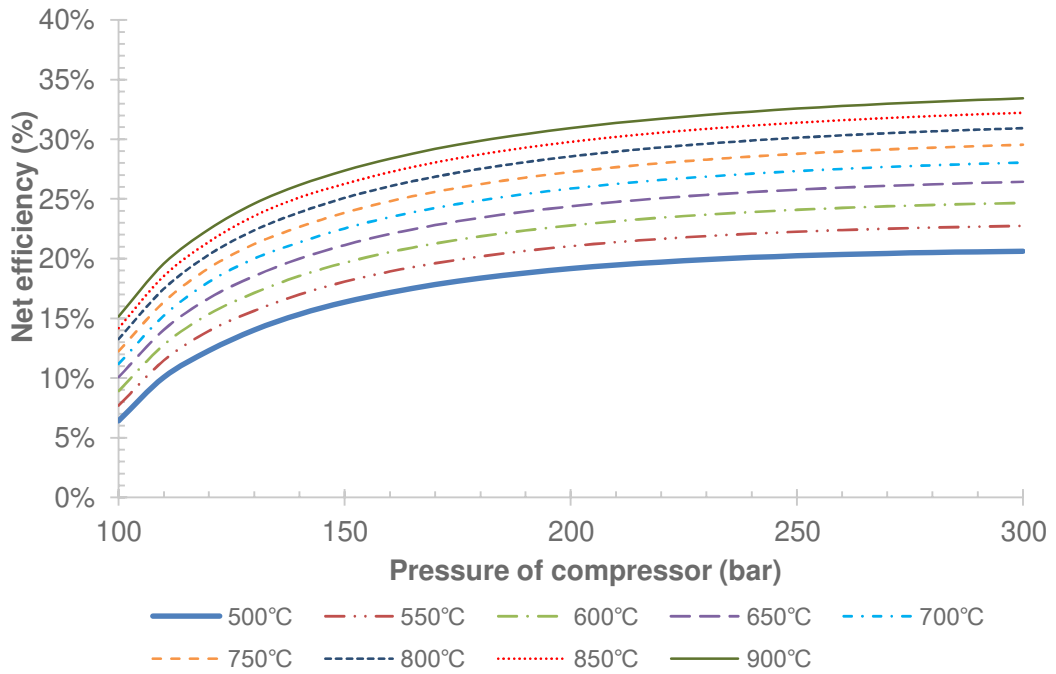
An analysis of the distribution of the auxiliary power consumption (Figure 2) has indicated that the ASU power consumption is the primary source of the efficiency penalty in all considered cases. In the sCO₂-coal case and the sCO₂-WP case, the ASU power consumption accounted for 13.7% and 14.4% of the gross power output, respectively. This corresponds to 46.2% and 44.5% of the auxiliary power consumption, respectively, and is in line with the results reported in the literature [56]. In addition, the CPU power requirement in these cases amounted to 38.6% and 37.7%, respectively.

Furthermore, an analysis of the specific fuel consumption revealed that its value in the sCO₂-WP case (830.99 g/kW_{el}h) is about 1.75 times that of the other two cases. This can be associated with the lower HHV of the wood pellet (16.8 MJ/kg) compared to that of coal (26.7 MJ/kg). Moreover, the specific CO₂ emissions were comparable in the SC-coal case (90.61 gCO₂/kW_{el}h) and the sCO₂-coal case (89.48 gCO₂/kW_{el}h), while the sCO₂-WP case led to a negative CO₂ emission (-1255.21 gCO₂/kW_{el}h) that corresponds to an atmospheric CO₂ removal rate of 3.70 MtCO₂ per annum. As a result, the sCO₂-WP case could offset CO₂ emissions from other processes with a potential benefit of an additional revenue stream from the emission trading system (ETS).

As mentioned above, the poorer performance of the cases with the sCO₂ cycle can be a result of non-optimised operating conditions. Figure 3 shows a positive correlation between net efficiency and both the TIT and the COP. As the COP increases from 250 bar to 300 bar at a TIT of 650°C, the net efficiency has increased from 28.10%_{HHV} to 28.78%_{HHV} in the sCO₂-coal case and from 25.78%_{HHV} to 26.43%_{HHV} in the sCO₂-WP case. Under a fixed amount of heat released from the oxy-combustion of fuel, the flow rate of the sCO₂ is reduced as the COP increases. Consequently, the energy consumption of the compressor and the amount of heat rejected in the cooler are reduced. These led to an increase in the net efficiency of the sCO₂ cases. However, the net efficiency gains are significantly smaller at pressures above 250 bar. This can be explained by an increase in the CO₂ density from 771.5 kg/m³ at 100 bar to 922.4 kg/m³ at 250 bar (~1 kg/(m³*bar) increase) and 948.0 kg/m³ at 300 bar (~0.5 kg/(m³*bar) increase). As a result, the increase in the energy requirement of the main compressor became close to the gains in the work output of the expander at higher pressures, resulting in lower gains in the net power output. Furthermore, Figure 3 reveals that an increase in the TIT from 650°C to 750°C, at a constant COP of 250 bar, increased the net efficiency from 28.10%_{HHV} to 31.25%_{HHV} in the sCO₂-coal case and from 25.78%_{HHV} to 28.78%_{HHV} in the sCO₂-WP case. Therefore, the sCO₂ cycle cases have the potential to offer superior net efficiency to the conventional steam cycle (28.55%_{HHV}) at higher TIT and COP values. It needs to be highlighted that, to maximise the net efficiency, the TIT should be as high as possible, considering material limitations.



(a)



(b)

Figure 3: Effect of the turbine inlet temperature and the pressure of compressor on the net efficiency in a) sCO₂-coal case and b) sCO₂-WP case

4.2 Economic assessment

The initial economic evaluation of the considered cases (Table 5) indicated that replacement of the conventional steam cycle (SC-coal case) with the sCO₂ cycle (sCO₂-coal case) resulted in a TCR

reduction of 20.1 M€. This was because of the lower capital cost of the sCO₂ cycle. This is reflected in a 4.1 €/kW_{el, net} reduction in the specific capital cost in the sCO₂-coal case. Importantly, on a change of fuel from coal (sCO₂-coal case) to wood pellets (sCO₂-WP case), the TCR was 57.4 M€ lower than that in the reference case. However, the specific capital cost increased by 130.4 €/kW_{el, net}, due to significantly lower net efficiency of the sCO₂-WP case compared to the SC-coal case.

The economic performance assessment has also revealed that, compared to the LCOE of the SC-coal case (88.3 €/MW_{el,h}), the values for the sCO₂-coal case and the sCO₂-WP case have increased by 0.6 €/MW_{el,h} (0.7%) and 31.8 €/MW_{el,h} (36.0%), respectively. Such an increase in the latter case is because of a 60.7% higher price for wood pellets (4.5 €/GJ) compared to that of coal (2.8 €/GJ) [21] (Figure 4) and lower net efficiency in the sCO₂-WP case (Table 5). As a result, the fuel component of the LCOE in the sCO₂-WP case is 76.9% higher than that in the sCO₂-coal case. Therefore, when the sCO₂-WP case is not considered to receive benefits from CO₂ offsetting, it is more economical to use coal rather than the wood pellets as fuel.

Table 5: Summary of economic performance

Parameter	Unit	SC-coal case	sCO ₂ -coal case	sCO ₂ -WP case
Gross power output	MW _{el}	659.45	652.26	621.77
Net power output	MW _{el}	466.17	458.79	420.96
Net electric efficiency	% _{HHV}	28.55	28.10	25.78
Fuel price	€/GJ	2.8	2.8	4.5
Total capital requirement	M€	1157.8	1137.7	1100.4
Specific capital cost	€/kW _{el, net}	2483.6	2479.5	2614.0
Annual fuel cost	M€/a	114.2	114.2	185.4
Annual fixed operating cost	M€/a	11.6	11.4	11.0
Annual variable operating cost	M€/a	47.0	46.6	47.9
Levelised cost of electricity	€/MW _{el,h}	88.3	88.9	120.1
CO ₂ avoided cost	€/tCO ₂	65.3	66.0	38.5

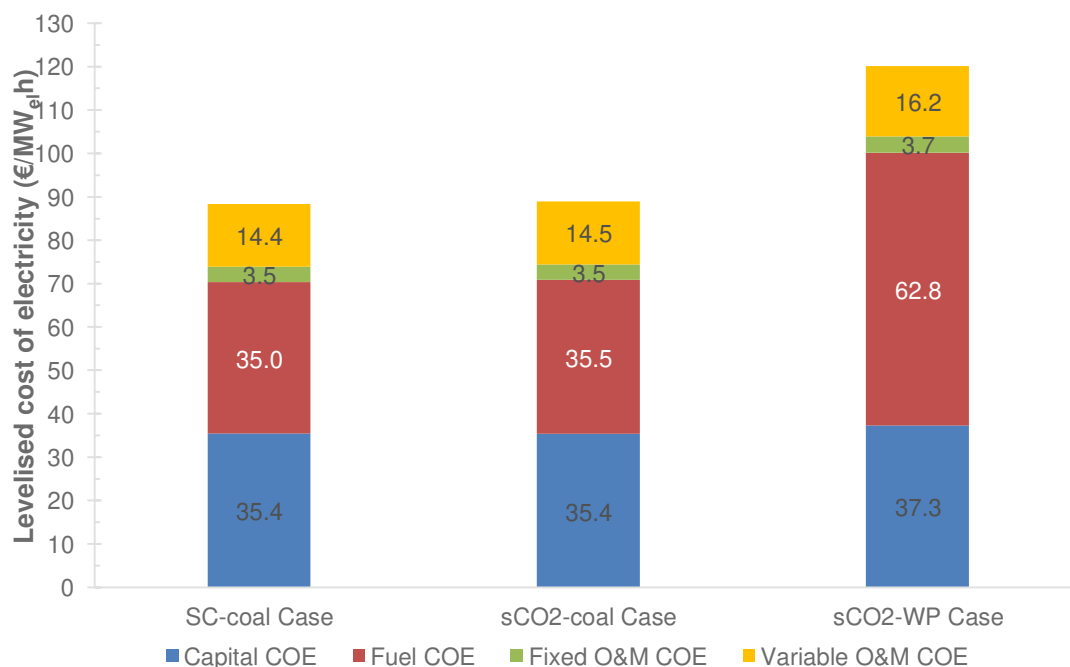
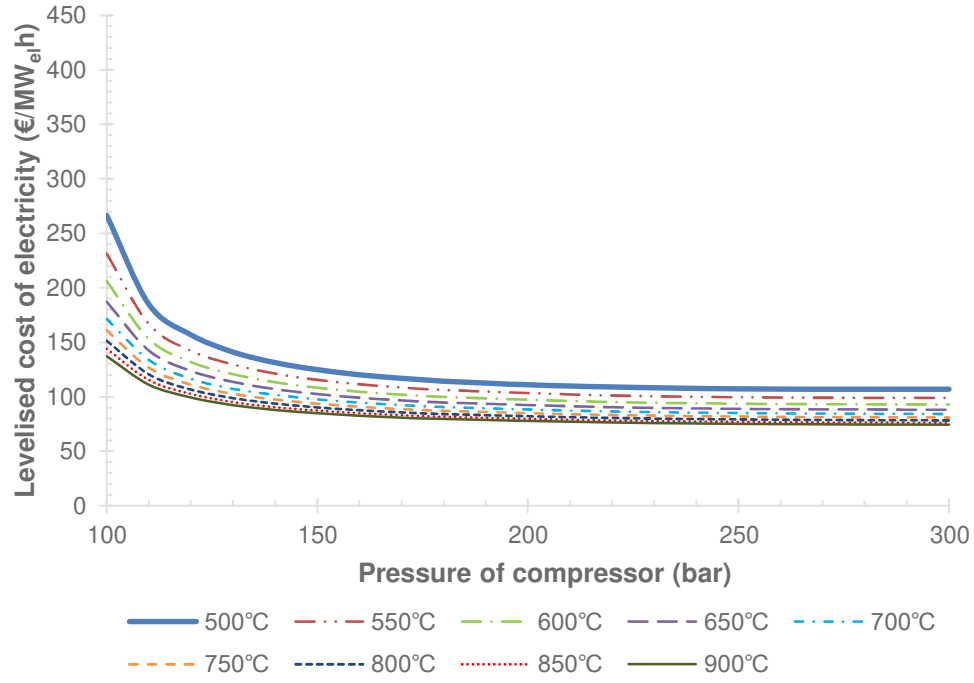


Figure 4: Distribution of levelised cost of electricity under initial assumptions

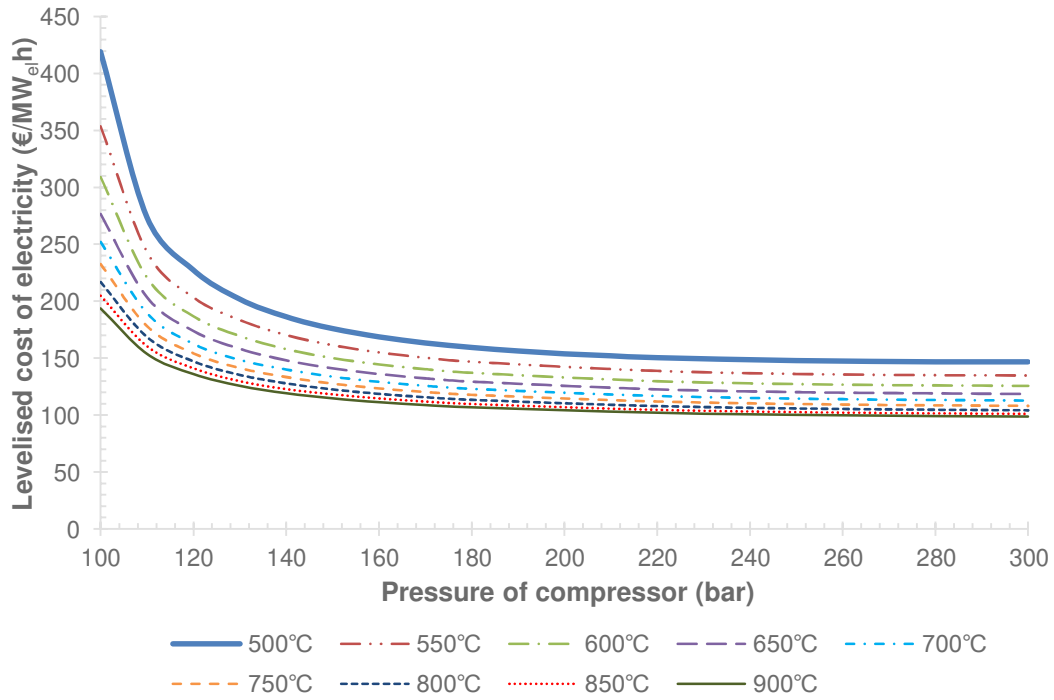
Although using wood pellets resulted in the LCOE higher by 31.8 €/kW_{el}h than that in the SC-coal case, analysis of the AC presented more favourable results that support BECCS deployment. Namely, the AC for the sCO₂-WP case was estimated to be 38.5 €/tCO₂, 41.1% lower than that of the SC-coal case (65.3 €/tCO₂). On the contrary, the AC of sCO₂-coal case was higher than the SC-coal case by 0.7 €/tCO₂ (1.1%). This can be explained primarily by negative CO₂ emissions in the sCO₂-WP case (-1255.21 gCO₂/kW_{el}h) compared to still positive CO₂ emissions in the other cases (~90 gCO₂/kW_{el}h). It can be expected, therefore, that BECCS may become favoured economically over the CCS systems considering the potential revenue from ETS, even though their net efficiencies are lower than that of CCS.

The results presented in Figure 5 and Figure 6 revealed that both the COP and the TIT are negatively correlated with the LCOE and the AC for coal and wood pellet fuels. This implies that an increase in both parameters will improve the economic performance of the considered cases. The trend could be correlated with the influence of the COP and the TIT on the net efficiency of considered cases, as presented in Figure 3. This means that the more efficient the power plant, the lower the LCOE and the lower the amount of emitted CO₂ when generating a kilowatt of electricity (e_{CO_2}). However, the largest reduction in both LCOE and AC are achieved at the lower end of the ranges considered for the COP and the TIT, whereas improvements above 250 bar and 700°C are relatively marginal.

Furthermore, due to a higher price of wood pellets compared to that of coal, the LCOE in the sCO₂-WP case is significantly higher than that of the sCO₂-coal case (Figure 5). This, subsequently, resulted in relatively poor performance of the sCO₂-WP case in the sensitivity analysis (Figure 5b). However, because the former case can achieve negative CO₂ emissions, a substantial difference in the AC was observed between the sCO₂-coal (Figure 6a) and the sCO₂-WP (Figure 6b) cases. This confirms that power plants based on BECCS can become more economically feasible than the CCS systems, achieving a competitive advantage in the market driven by carbon tax prices.

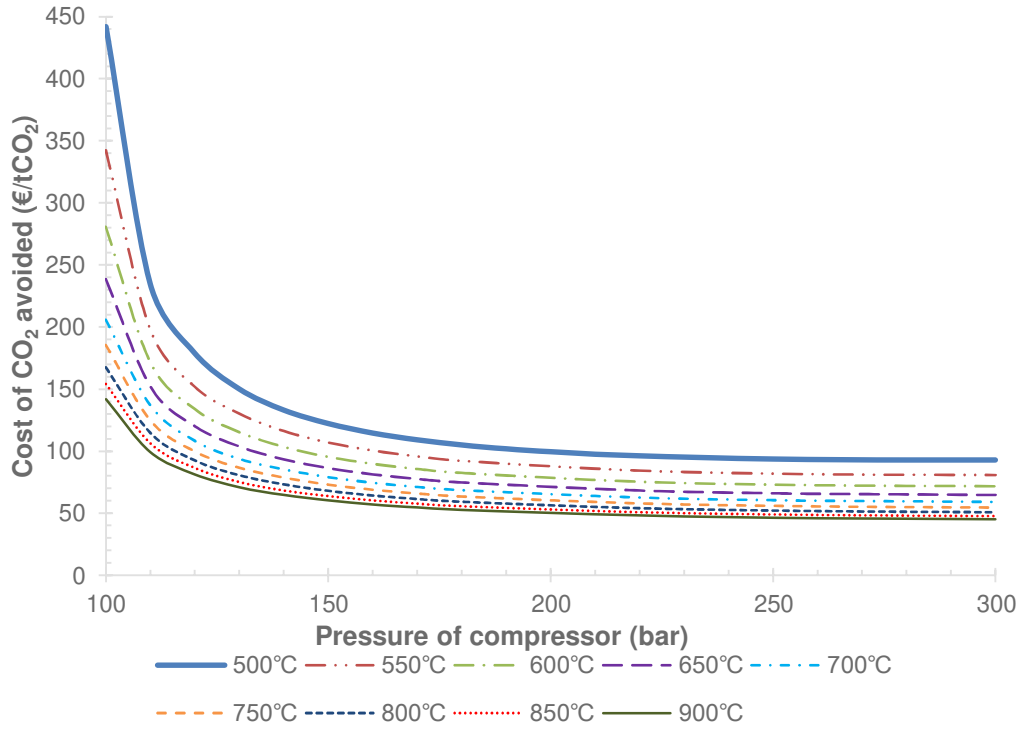


(a)

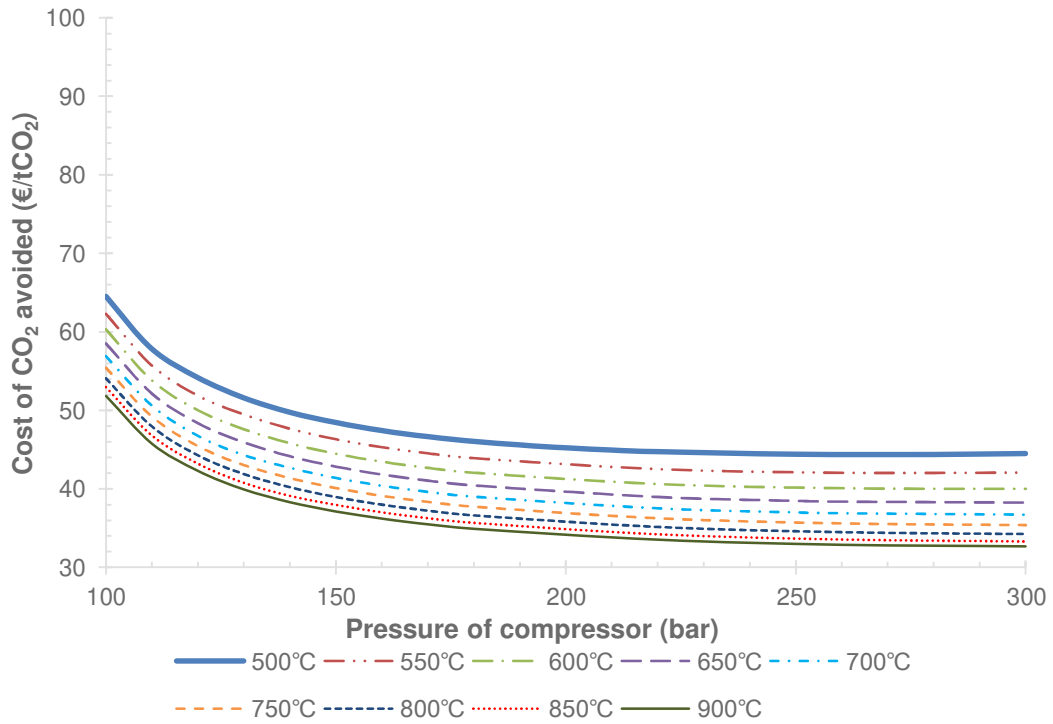


(b)

Figure 5: Effect of the turbine inlet temperature and the pressure of compressor on the levelised cost of electricity in a) sCO₂-coal case and b) sCO₂-WP case



(a)



(b)

Figure 6: Effect of the turbine inlet temperature and the pressure of compressor on the cost of CO₂ avoided in a) oxy-fuel combustion coal-fired power plant with sCO₂ cycle and b) oxy-fuel combustion biomass-fired power plant with sCO₂ cycle

To understand the benefits of BECCS over CCS in the market driven by the carbon tax, the effect of the carbon tax on the economic performance of sCO₂-coal and sCO₂-WP cases has been evaluated (Figure 7). This analysis has revealed that the parity of LCOE will be achieved for both cases at the carbon tax of 23.18 €/tCO₂. Such a result indicates that when the carbon tax is more than 23.18 €/tCO₂, the sCO₂-WP case is more economically favoured. Importantly, with the current CO₂ price of European emission allowance of 23.74 €/tCO₂ [57], the sCO₂-WP case would be a more economically feasible option. Moreover, if the carbon tax is 95.70 €/tCO₂, the revenue generated by offsetting CO₂ emissions in the sCO₂-WP results in a LCOE of zero.

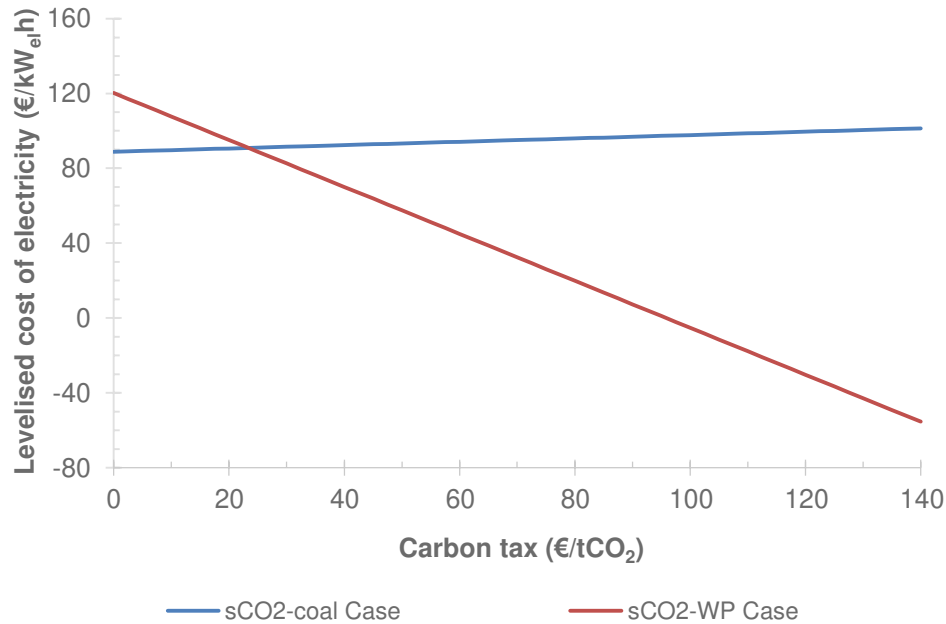


Figure 7: Effect of the carbon tax on the levelised cost of electricity

Furthermore, it is pertinent to assess the effect of the economic assumptions made in Table 3 on the economic performance of the considered cases. Figure 8 reveals that the fuel price significantly influences both the LCOE and the AC. On a 25% increase in the fuel price, the LCOE of the sCO₂-WP case increased by 35.4% (141.1 €/MW_eh), a significantly higher increase than that in the sCO₂-coal case, for which the LCOE has increased by 17.8% (104.7 €/MW_eh). Importantly, even if the price of wood pellets and coal are comparable, between 3.0–4.0 €/GJ, the LCOE of the sCO₂-WP case was found to be higher than that of the sCO₂-coal case by 7.3–8.4 €/MW_eh. This was primarily due to the lower net efficiency of the sCO₂-WP case. Furthermore, even though the price of coal is lower, the AC of the sCO₂-coal case is much higher than that of the sCO₂-WP case (Figure 8). This is due to negative CO₂ emissions in the sCO₂-WP case. Moreover, a variation in the coal price has a greater impact on the AC than that in the wood pellet price. This indicates a potentially higher resilience of BECCS to uncertainty in the future energy market.

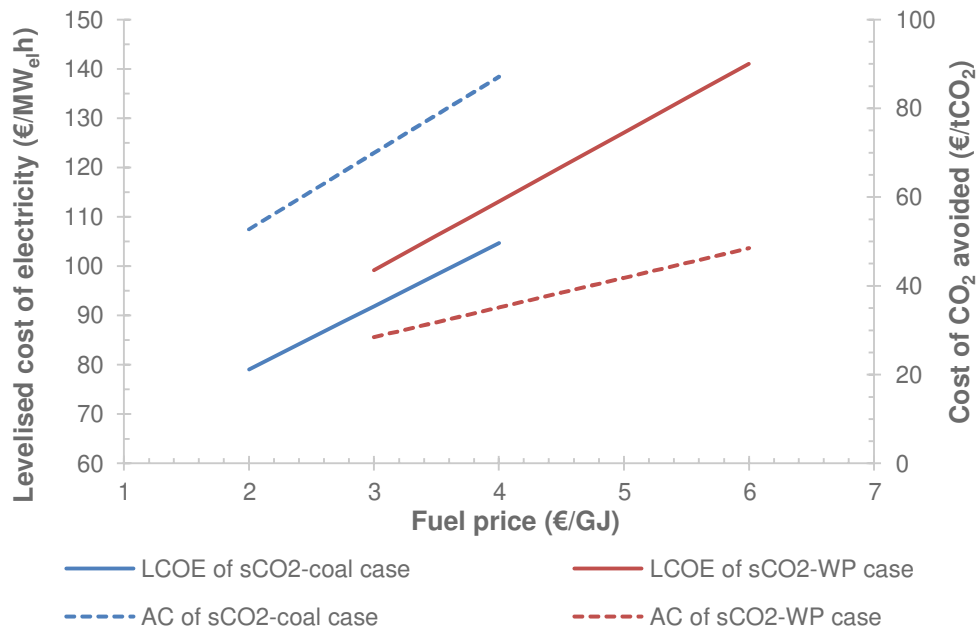


Figure 8: The effect of the fuel price on the levelised cost of electricity and the cost of CO₂ avoided

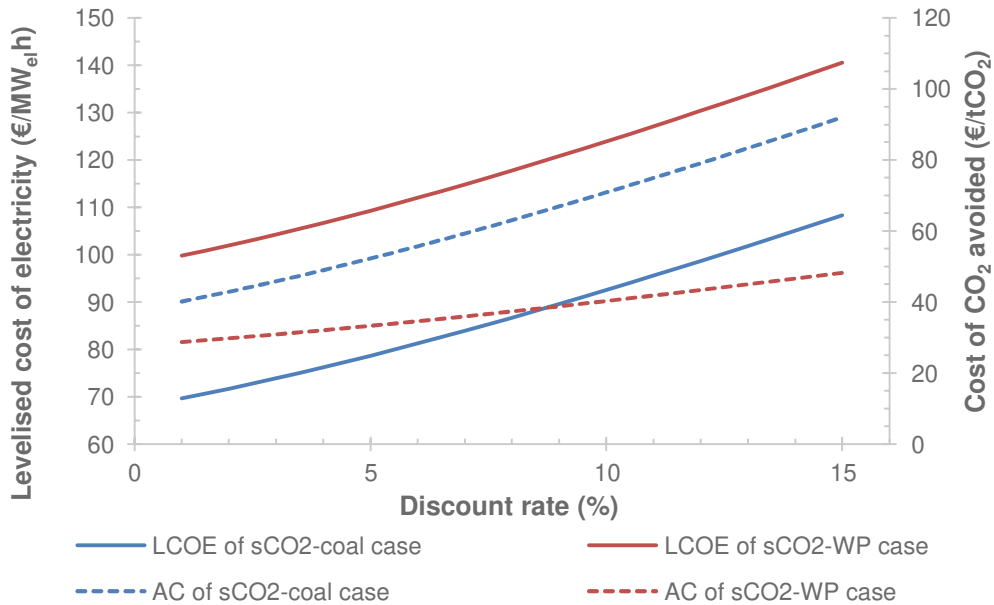


Figure 9: The effect of the discount rate on the levelised cost of electricity and the cost of CO₂ avoided

Finally, the results presented above were determined based on a discount rate of 8.78% (Table 3). As this figure depends on the level of risk associated with the project and directly influences the considered economic performance indicators, it is pertinent to assess its impact on the economic feasibility of the considered cases. Figure 9 revealed that an increase in the discount rate will result in a subsequent increase in the LCOE. Importantly, the observed trend is comparable for both sCO₂-coal and sCO₂-WP cases. On the contrary, Figure 9 indicated that the AC in the former case is more sensitive

to an increase in the discount rate, with rather low sensitivity in the sCO₂-WP case. This indicates that the BECCS systems may be less sensitive to the risks associated with the project delivery.

4.3 Feasibility assessment

Considering the outcome of the initial techno-economic assessment and corresponding sensitivity analyses, the potential for further improvement in the performance of the oxy-fuel combustion power plant with the sCO₂ cycle has been indicated. Therefore, the techno-economic feasibility of the considered cases has been evaluated under the revised conditions (Table 6), considering the outputs from the sensitivity analyses. These indicated that substantial improvements in the economic performance occurred until the TIT and COP reached 700°C and 250 bar, respectively. Under such operating conditions, the net efficiency of both the sCO₂-coal and sCO₂-WP case increased by around 1.6%_{HHV} points. Compared to the SC-coal case, the net efficiency under revised conditions was 1.2%_{HHV} points higher for the sCO₂-coal case and 0.5%_{HHV} points lower for the sCO₂-WP case. An increase in the COP to 300 bar resulted in a further gain in the net efficiency of 0.8%_{HHV} points (sCO₂-coal case) and 0.7%_{HHV} points (sCO₂-WP case). Overall, an increase in the operating conditions has reduced the efficiency penalty to 8.3%_{HHV} points (sCO₂-coal case) and 10.8%_{HHV} points (sCO₂-WP case) with respect to the coal-fired power plant without CO₂ capture. This implies that the former case is superior to the reference SC-coal case (10.3%_{HHV} points), but the thermodynamic performance of the latter is still inferior.

From the economic feasibility perspective, an increase in the TIT and COP to 700°C and 250 bar, respectively, resulted in significant improvements in the economic performance of the sCO₂-coal case (Table 6). Namely, the LCOE reduced from 88.9 €/MW_eh to 85.1 €/MW_eh and the AC reduced from 66.0 €/tCO₂ to 60.5 €/tCO₂, both of which are below the figures reported for the SC-coal case. Further reductions by 0.9 €/MW_eh and 1.4 €/tCO₂, respectively, were obtained on an increase of the COP to 300 bar. In addition, some improvement in the economic performance of the sCO₂-WP case was also observed. However, this improvement was less pronounced than that in the sCO₂-coal case. This is because although a 4.7% reduction in the LCOE was achieved on an increase in the TIT and COP to 700°C and 250 bar, it is still substantially higher (114.4 €/MW_eh) than that of the other considered cases (Table 6). Although the LCOE in the sCO₂-WP case was 33-35% higher than that for the sCO₂-coal case, this increase is lower than that reported by Al-Qayim et al. [29] for oxy-fuel combustion power plants with a conventional steam cycle. It also needs to be emphasised that even though the sCO₂-WP case was characterised with the lowest net efficiency, it had the lowest AC among the considered cases. Therefore, as discussed above, the main benefit of BECCS that makes it economically feasible relies on its inherent ability to operate with negative CO₂ emissions, subsequently offsetting CO₂ emissions from other sources that are difficult to decarbonise, such as the aviation or transportation sectors. Nevertheless, without the revenue from the carbon tax, the relatively poor techno-economic performance of the sCO₂-WP case compared to the other cases would not support commercialisation of BECCS.

Table 6: Summary of the techno-economic assessment

Parameter	Unit	SC-coal case	sCO ₂ -coal case				sCO ₂ -WP case	
Turbine inlet temperature	°C	537	650	700	700	650	700	700
Compressor outlet pressure	bar	235	250	250	300	250	250	300
Gross power output	MW _{el}	659.4	652.3	679.1	691.4	621.8	647.3	659.0
Net power output	MW _{el}	466.17	458.8	485.5	497.8	421.0	446.4	458.0
Total capital requirement	M€	1157.8	1137.7	1164.7	1196.1	1100.4	1127.4	1157.7
Specific capital cost	€/kW _{net}	2483.6	2479.5	2398.8	2403.0	2614.0	2525.6	2527.6
CO ₂ emission rate	kg/s	11.7	11.4	11.4	11.4	-146.8	-146.8	-146.8
	MtCO ₂ /a	0.30	0.29	0.29	0.29	-3.70	-3.70	-3.70
η_{net}	% _{HHV}	28.55	28.10	29.73	30.48	25.78	27.34	28.05
η_{gross}	% _{HHV}	40.38	39.95	41.59	42.34	38.08	39.64	40.36
Net efficiency penalty	% _{HHV}	10.3	10.7	9.1	8.3	13.0	11.5	10.8
LCOE	€/MW _{el} h	88.3	88.9	85.1	84.2	120.1	114.4	112.7
AC	€/tCO ₂	65.3	66.0	60.5	59.1	38.5	37.0	36.7

5 Conclusions

This study presented an investigation of the techno-economic performance of the novel oxy-combustion coal- and biomass-fired power plant with the sCO₂ cycle and compared this with the reference oxy-combustion coal-fired power plant with the conventional steam cycle. This study has proved that:

- replacement of the conventional steam cycle (SC-coal case) with the sCO₂ cycle (sCO₂-coal case) resulted in a reduction in the net efficiency by 0.4%_{HHV} and an increase in the LCOE by 0.6 €/MW_{el}h;
- replacement of the fuel from coal (sCO₂-coal case) to wood pellets (sCO₂-WP case) resulted in a further reduction in the net efficiency of 2.3%_{HHV} and an increase in the LCOE of 31.2 €/MW_{el}h but enabled achieving a substantial negative CO₂ emission of 1255.2 gCO₂/kW_{el}h.
- compared to the reference case, the sCO₂-WP case had better environmental performance, but had poorer thermodynamic and economic performance under the initial conditions with no carbon tax considered. Therefore, deployment of BECCS relies on the development of an efficient CO₂ market that will support carbon-negative technologies.
- potential improvements in the techno-economic performance are achievable by increasing the TIT and COP. Both parameters were positively correlated with the net efficiency and negatively correlated with the LCOE and AC. Moreover, fuel prices and discount rate were shown to be positively correlated with LCOE and AC.

- the sCO₂-coal case will result in a 2%_{HHV} points higher net efficiency and 4.1 €/MW_{el}h lower LCOE than that for reference SC-coal case. As this study utilised a simple recuperated sCO₂ cycle, such outcome confirms that implementation of advanced power cycles can substantially reduce the economic and efficiency penalties associated with CCS; and
- inherent ability of the sCO₂-WP case to operate with negative CO₂ emissions was shown to offset the increased efficiency penalty when the carbon tax was above 23.18 €/tCO₂. Above this value of the carbon tax, the sCO₂-WP case became more economically feasible than the sCO₂-coal case. Moreover, if the carbon tax was above 95.70 €/tCO₂, the revenue associated with offsetting the CO₂ emissions resulted in a LCOE below zero.

References

1. IEA. Global Energy and CO₂ Status Report. The latest trends in energy and emissions in 2018. Paris, France: IEA Publications; 2019.
2. Masson-Delmotte V., Zhai P., Pörtner H-O., Roberts D., Skea J., Shukla P R., Pirani A., Moufouma-Okia W., Péan C., Pidcock R., Connors S., Matthews J B R., Chen Y., Zhou X., I. Gomis M., Lonnoy E., Maycock T., Tignor M., Waterfield T. Global warming of 1.5°C. Report of the Intergovernmental Panel on Climate Change. Geneva, Switzerland; 2018. Available at: https://report.ipcc.ch/sr15/pdf/sr15_spm_final.pdf. IEA. Global action to advance carbon capture and storage - a focus on industrial applications. France; 2013.
4. GCCSI. Global status of CCS 2017. Docklands, Australia; 2017. Available at: <https://www.globalccsinstitute.com/wp-content/uploads/2018/12/2017-Global-Status-Report.pdf>.
5. Abraham BM., Asbury JG., Lynch EP., Teotia APS. Coal-oxygen process provides carbon dioxide for enhanced recovery. Oil & Gas Journal. 1982; 80(11): 68–70.
6. Horn FL., Steinberg M. Control of carbon dioxide emissions from a power plant (and use in enhanced oil recovery). Fuel. 1982; 61(5): 415–422. DOI:10.1016/0016-2361(82)90064-3
7. Payne R., L Chen S., Wolsky AM., Richter WF. CO₂ recovery via coal combustion in mixtures of oxygen and recycled flue gas. Combustion Science and Technology. September 1989; 67(1–3): 1–16. DOI: 10.1080/00102208908924058
8. Woycenko DM., Van de Kamp WL., Roberts PA. Summary of the APG research program. Combustion of pulverised coal in a mixture of oxygen and recycled flue gas. 1st edn. Ijmuiden, the Netherlands: Elsevier; 1995. DOI: 10.1016/C2013-0-19301-4
9. Fujimori T., Yamada T. Realization of oxyfuel combustion for near zero emission power generation. Proceedings of the Combustion Institute. 2013; 34(2): 2111–2130. DOI: 10.1016/j.proci.2012.10.004
10. Tan Y., Croiset E., Douglas MA., Thambimuthu K V. Combustion characteristics of coal in a mixture of oxygen and recycled flue gas. Fuel. 2006; 85(4): 507–512. DOI: 10.1016/j.fuel.2005.08.010
11. Rathnam RK., Elliott L., Moghtaderi B., Gupta R., Wall T. Differences in coal reactivity in air and oxy-fuel conditions and implications for coal burnout. Proceedings of the 31st International Conference on Coal Utilization and Fuel Systems. Florida, United States, May, 2006.
12. Douglas MA., Chui E., Tan Y., Lee GK., Croiset E., Thambimuthu KV. Oxy-fuel combustion at the CANMET vertical combustor research facility. Washington DC, USA, 2001.
13. Croiset E., Thambimuthu K V. NO_x and SO₂ emissions from O₂/CO₂ recycle coal combustion. Fuel. 2001; 80(14): 2117–2121. DOI: 10.1016/S0016-2361(00)00197-6
14. Boot-Handford ME., Abanades JC., Anthony EJ., Blunt MJ., Brandani S., Mac Dowell N., Fernández JR., Ferrari MC., Gross R., Hallett JP., Haszeldine RS., Heptonstall P., Lyngfelt A., Makuch Z., Mangano E., Porter RTJ., Pourkashanian M., Rochelle GT., Shah N., Yao JG., Fennell PS. Carbon capture and storage update. Energy and Environmental Science. 2014; 7: 130–189. DOI: 10.1039/C3EE42350F
15. Strömberg L., Lindgren G., Jacoby J., Giering R., Anheden M., Burchhardt U., Altmann H.,

- Kluger F., Stamatelopoulos G.-N. Update on Vattenfall's 30 MW_{th} oxyfuel pilot plant in Schwarze Pumpe. *Energy Procedia*. 2009; 1(1): 581–589. DOI: 10.1016/j.egypro.2009.01.077
16. Ochs T., Oryshchyn D., Woodside R., Summers C., Patrick B., Gross D., Schoenfeld M., Weber T., O'Brien D. Results of initial operation of the Jupiter Oxygen Corporation oxy-fuel 15 MW_{th} burner test facility. *Energy Procedia*. 2009; 1(1): 511–518. Available at: DOI:10.1016/j.egypro.2009.01.068
 17. McDonald DK., Flynn TJ., DeVault DJ., Varagani R., Levesque S., Castor W. MWt clean environment development oxy-coal combustion test program. The 33rd International Technical Conference on Coal Utilization and Fuel Systems. Clearwater, Florida, USA; 2008.
 18. Hesselmann G., Cameron ED., Sturgeon DW., McGhie C., Fitzgerald FD. Oxyfuel firing and lessons learned from the demonstration of a full-sized utility scale 40MW oxycoal combustion system. South African Carbon Capture And Storage Conference. Johannesburg, South Africa; 2009.
 19. Cook PJ. Demonstration and deployment of carbon dioxide capture and storage in Australia. *Energy Procedia*. 2009; 1(1): 3859–3866. DOI: 10.1016/j.egypro.2009.02.188
 20. Spero C., Yamada T. Callide Oxyfuel Project Final Results. Fortitude Valley, Queensland, Australia; 2018. Available at: <https://www.globalccsinstitute.com/archive/hub/publications/202090/cop-finalresults-publicreport-march2018.pdf>
 21. Cormos CC. Oxy-combustion of coal, lignite and biomass: A techno-economic analysis for a large scale Carbon Capture and Storage (CCS) project in Romania. *Fuel*. 2016; 169: 50–57. DOI:10.1016/j.fuel.2015.12.005
 22. Hanak DP., Powell D., Manovic V. Techno-economic analysis of oxy-combustion coal-fired power plant with cryogenic oxygen storage. *Applied Energy*. 2017; 191: 193–203. DOI:10.1016/j.apenergy.2017.01.049
 23. Singh D., Croiset E., Douglas P., Douglas M. Techno-economic study of CO₂ capture from an existing coal-fired power plant: MEA scrubbing vs. O₂/CO₂ recycle combustion. *Energy Conversion and Management*. 2003; 44(19): 3073–3091. DOI: 10.1016/S0196-8904(03)00040-2
 24. Tola V., Cau G., Ferrara F., Pettinau A. CO₂ emissions reduction from coal-fired power generation: a techno-economic comparison. *Journal of Energy Resources Technology*. 2016; 138(6). DOI: 10.1115/1.4034547
 25. Zhou C., Shah K., Moghtaderi B. Techno-economic assessment of integrated chemical looping air separation for oxy-fuel combustion: an Australian case study. *Energy & Fuels*. 2015; 29(4): 2074–2088. DOI: 10.1021/ef5022076
 26. Ackiewicz M., Litynski J., Kemper J., Berenblyum R., Deich N. Technical summary of bioenergy carbon capture and storage (BECCS). Washinton DC, USA: Carbon Sequestration Leadership Forum; 2018. Available at: https://www.cslforum.org/cslf/sites/default/files/documents/Publications/BECCS_Task_Force_Report_2018-04-04.pdf.
 27. Drax. Carbon dioxide now being captured in first of its kind BECCS pilot - Drax Group. 2019. Available at: https://www.drax.com/press_release/world-first-co2-beccs-ccus/
 28. Kraxner F., Fuss S., Krey V., Best D., Leduc S., Kindermann G., Yamagata Y., Schepaschenko D.,

- Shvidenko A., Aoki K., Yan J. The role of bioenergy with carbon capture and storage (BECCS) for climate policy. *Handbook of Clean Energy Systems*. Chichester, UK: John Wiley & Sons; 2015. 1–19. DOI: 10.1002/9781118991978.hces049
29. Al-Qayim K., Nimmo W., Pourkashanian M. Comparative techno-economic assessment of biomass and coal with CCS technologies in a pulverized combustion power plant in the United Kingdom. *International Journal of Greenhouse Gas Control*. 2015; 43: 82–92. DOI: 10.1016/j.ijggc.2015.10.013
 30. Feher EG. The supercritical thermodynamic power cycle. *Energy Conversion*. 1968; 8(2): 85–90. DOI: 10.1016/0013-7480(68)90105-8
 31. Zada KR., Kim R., Wildberger A., Schalansky CP. Analysis of supercritical CO₂ Brayton cycle recuperative heat exchanger size and capital cost with variation of layout design. The 6th International Supercritical CO₂ Power Cycles Symposium. Pittsburgh, USA, 2018.
 32. Angelino G. Carbon dioxide condensation cycles for power production. *ASME Journal of Engineering for Power*. 1968; 90(3): 287–296. DOI: 10.1115/1.3609190
 33. Gokhshtein DP., Verkhivker GP. Use of carbon dioxide as a heat carrier and working substance in atomic power stations. *Soviet Atomic Energy*. 1969; 26(4): 430–432. DOI: 10.1007/bf01371881
 34. Dostal V., Driscoll MJ., Hejzlar P. A supercritical carbon dioxide cycle for next generation nuclear reactors. Cambridge, MA, USA: Massachusetts Institute of Technology; 2004. Available at: <http://hdl.handle.net/1721.1/17746>
 35. Delene JG., Hudson CR. Cost estimates guidelines for advanced nuclear power technologies. USA: Oak Ridge National Laboratory; 1993. Available at: https://inis.iaea.org/collection/NCLCollectionStore/_Public/25/011/25011638.pdf
 36. ABB/Combustion Engineering Inc., Bechtel National Inc., Gas-Cooled Reactor Associates., General Atomics., Oak Ridge National Laboratory., Stone & Webster Engineering Corp. Modular high temperature gas-cooled reactor commercialization and generation cost estimates. Gas-Cooled Reactor Associates; 1993. Available at: <https://www.osti.gov/servlets/purl/10198837>
 37. Hanak DP., Manovic V. Calcium looping with supercritical CO₂ cycle for decarbonisation of coal-fired power plant. *Energy*. 2016; 102: 343–353. DOI: 10.1016/j.energy.2016.02.079
 38. Hanak DP., Jenkins BG., Kruger T., Manovic V. High-efficiency negative-carbon emission power generation from integrated solid-oxide fuel cell and calciner. *Applied Energy*. 2017; 205: 1189–1201. DOI: 10.1016/j.apenergy.2017.08.090
 39. Bloomberg., International Coal Report., World Bank. Coal, South African export price - Monthly Price - Commodity Prices - Price Charts, Data, and News. IndexMundi. 2019. Available at: <https://www.indexmundi.com/commodities/?commodity=coal-south-african&months=60¤cy=eur>.
 40. Korhaliller S. The UK's biomass energy development path. London, UK, 2010. Available at: <http://pubs.iied.org/pdfs/G02921.pdf>
 41. Fout T., Zoelle A., Keairns D., Turner M., Woods M., Kuehn N., Shah V., Chou V., Pinkerton L. Cost and performance baseline for fossil energy plants volume 1a: bituminous coal (PC) and natural gas to electricity. Pittsburgh, PA, USA: National Energy Technology Laboratory; 2015.
 42. Michalski S., Hanak DP., Manovic V. Techno-economic feasibility assessment of calcium

- looping combustion using commercial technology appraisal tools. *Journal of Cleaner Production*. 2019; 219: 540–551. DOI: 10.1016/j.jclepro.2019.02.049
43. Aspen Technology Inc. Aspen Plus V10 help: General Coal Enthalpy Model. Bedford, USA; 2017. Available at: <http://www.aspentech.com>
 44. Rubin E., Booras G., Davison J., Ekstrom C., Matuszewski M., McCoy S., et al. Toward a common method of cost estimation for CO₂ capture and storage at fossil fuel power plants. 2013; 1–36. Available at: <http://cdn.globalccsinstitute.com/sites/default/files/publications/85761/toward-common-method-cost-estimation-ccs-fossil-fuel-power-plants-white-paper.pdf>
 45. Green DW., Perry RH. *Perry's Chemical Engineers' Handbook*. 8th edn. USA: The McGraw-Hill Companies, Inc.; 2008. Available at: <https://www.accessengineeringlibrary.com/browse/perrys-chemical-engineers-handbook-eighth-edition>
 46. Benjelloun M., Doulgeris G., Singh R. A method for techno-economic analysis of supercritical carbon dioxide cycles for new generation nuclear power plants. *Proceedings of the Institution of Mechanical Engineers, Part A: Journal of Power and Energy*. 2012; 226: 372–383. DOI: 10.1177/0957650911429643
 47. Criado YA., Arias B., Abanades JC. Calcium looping CO₂ capture system for back-up power plants. *Energy and Environmental Science*. 2017; 10: 1994–2004. DOI: 10.1039/c7ee01505d
 48. Gabbriellini R., Singh R. Economic and scenario analyses of new gas turbine combined cycles with no emissions of carbon dioxide. *Journal of Engineering for Gas Turbines and Power*. 2005; 127: 531. DOI: 10.1115/1.1850492
 49. Massachusetts Institute of Technology. CoolProp. 2019. Available at: <http://www.coolprop.org/>
 50. Hanak DP., Manovic V. Combined heat and power generation with lime production for direct air capture. *Energy Conversion and Management*. 2018; 160: 455–466. DOI:10.1016/j.enconman.2018.01.037
 51. Porta FL. Technical and economical analysis of future perspectives of solar thermal power plants. University of Padua; 2006;
 52. Ciferno J., Haslbeck J., Black J., Kuehn N., Lewis E., Rutkowski M. *Pulverized Coal Oxycombustion Power Plants Volume 1 : Bituminous Coal to Electricity Final Report*. Pittsburgh, PA, USA: National Energy Technology Laboratory; 2008.
 53. Yang Y., Zhai R., Duan L., Kavosh M., Patchigolla K., Oakey J. Integration and evaluation of a power plant with a CaO-based CO₂ capture system. *International Journal of Greenhouse Gas Control*. 2010; 4(4): 603–612. DOI: 10.1016/j.ijggc.2010.01.004
 54. Martínez A., Lara Y., Lisbona P., Romeo LM. Operation of a mixing seal valve in calcium looping for CO₂ capture. *Energy and Fuels*. 2014; 28(3): 2059–2068. DOI: 10.1021/ef402487e
 55. Mendez C., Rochau G. *sCO₂ Brayton Cycle: Roadmap to sCO₂ power cycles commercial applications*. California, USA: Sandia National Laboratories; 2018. Available at: <https://prod.sandia.gov/techlib-noauth/access-control.cgi/2018/186187.pdf>
 56. Maddahi L., Hossainpour S. Thermo-economic evaluation of 300 MW coal based oxy-fuel power plant integrated with organic Rankine cycle. *International Journal of Greenhouse Gas Control*. 2019; 88: 383–392. DOI: 10.1016/j.ijggc.2019.07.004

57. Market Insider. CO₂ european emission allowances spot price chart. 2019. Available at: <https://markets.businessinsider.com/commodities/co2-european-emission-allowances>.

Techno-economic assessment of coal- or biomass-fired oxy-combustion power plants with supercritical carbon dioxide cycle

Wei, Xiaoyu

2020-07-10

Attribution-NonCommercial-NoDerivatives 4.0 International

Wei X, Manovic V, Hanak D. (2020) Techno-economic assessment of coal- or biomass-fired oxy-combustion power plants with supercritical carbon dioxide cycle. *Energy Conversion and Management*, Volume 221, October 2020, Article number 113143

<https://doi.org/10.1016/j.enconman.2020.113143>

Downloaded from CERES Research Repository, Cranfield University